SOIL-FOUNDATION-STRUCTURE BEHAVIOR AT THE OAKLAND OUTER HARBOR WHARF

G. Norris and R. Siddharthan
Associate Professors, University of Nevada, Reno

Z. Zafir, S. Abdel-Ghaffar, and P. Gowda
Graduate Students, University of Nevada, Reno

ABSTRACT

This paper discusses the use of CSMIP records at Oakland Outer Harbor Wharf (along with that from Yerba Buena) to study the free-field motions at Oakland Outer Harbor, both at shallow depth and to bedrock, and the possible softening of soils surrounding the piles supporting the instrumented wharf. The paper also discusses the determination of the motion on the instrumented wharf using free-field motion input and deflection compatible lateral and vertical pile foundation stiffnesses. Such derived motion compares well with the recorded motions on the deck. While there was no reported liquefaction at the site, there was at nearby locations; and the consequence of an assumed lower relative density of the near-surface sand at Oakland Outer Harbor is discussed. Likewise, the consequence of a change in the orientation of the wharf or the incoming motions, assessed by interchanging the direction of the free-field motions, is presented. These latter changes reflect conditions under which a soil-foundation interaction failure or structural failure of the batter piles may have developed, failures that occurred at facilities nearby.

INTRODUCTION

During the Loma Prieta earthquake of October 17, 1989, there was considerable damage to facilities at Oakland harbor; however, there was no specific failure of the soil or damage to the structure of the CSMIP instrumented wharf (Berths 24,25,26) at Oakland Outer Harbor. This paper discusses the use of CSMIP records at the Oakland Outer Harbor Wharf to assess free-field motions in the soil supporting the piles of the wharf, the nonlinear variation in inertial interaction stiffnesses of the piles (with due consideration of free field strain and any softening due to developing pore pressures associated with unrealized liquefaction), and the assessed motion on the deck using free-field input through deflection compatible equivalent linear foundation springs. In addition, the paper discusses the consequence of a decrease in the relative density of the near-surface sand layer supporting the piles or the direction of incoming motions. Such changes reflect conditions under which there may have been liquefaction or a soil-foundation interaction failure or structural failure of the batter piles as observed at nearby facilities.

LAYOUT OF RECORDING INSTRUMENTS AND SOIL PROFILE

Figure 1 presents the layout of the instrumentation at Oakland Outer Harbor Wharf. Channels 1, 3, 10 and 12 are the horizontal free-field instruments located to the east of the wharf. They exhibited peak accelerations of 0.28g, 0.22g, 0.27g, and 0.29g, respectively, during the Loma Prieta earthquake.

Figure 2 represents the averaged soil profile used for the horizontal free-field response evaluation as constructed based on soil and geophysical data taken from a number of sources (see Acknowledgements).

SHEAR MODULUS AND DAMPING CURVES FOR THE SOIL LAYERS

In performing an equivalent linear one-dimensional ground response analysis using the commonly employed program, SHAKE (Schnabel et al., 1972), it is necessary to specify the soil type (SAND, CLAY or ROCK) and to supply the shear modulus reduction (G/G_{max}) and damping (β) curves for these materials. In the deep deposit considered here (approximately 495 ft. to Franciscan greywacke), the vertical effective stress σ'_{vo} increases to over 25000 lb/ft^2. There have been a number of laboratory studies, e.g., that by Hardin and Drnevich (1972), that have shown a dependency of G/G_{max} and β values on the level of σ'_{vo}. Therefore, a modified SHAKE analysis was used here in which such dependency was modeled.

Figure 3 shows curves for Bay Mud modified from the curves given by Seed and Sun (1989) using a relationship for overburden pressure established from the work of Hardin and Drnevich (1972). It should be noted that the Seed and Sun shear modulus curve for Bay Mud (σ'_{vo}=2000 lbs/ft^2) exhibits linearity (i.e., G/G_{max}=1) up to a greater strain ($1x10^{-2}$%) than that for other clays and a damping curve that falls near the lower range for the average of all clays (see Seed and Idriss, 1970). Similar stress-dependent modulus and damping curves were derived for sands as shown in Figure 4.

FREE FIELD RESPONSE

All free-field horizontal acceleration histories (Channels 1, 3, 10 and 12) were considered separately, and the motions at the top of the bedrock at a depth of 495 ft. were computed using deconvolution. Figure 5 shows the spectral acceleration curve for rock motion derived using the modified SHAKE program along with the spectral curve for the particular (ground surface) input motion for Channels 10 and 12. (The curves for Channel 1 are like those for Channel 10; and 3 like those 12.) One will note that the predominant period of base and surface motions is about 0.6 to 0.8 seconds and that the spectrum for motion in the long direction of the wharf (Channels 12 and 3) is wider indicating energy input over a wider range in frequency than that for motions transverse to the wharf (Channels 10 and 1). This raises the question of the possibility for damage to the wharf had the orientation of the wharf or the incoming motions been reversed.

The influence of the soil deposit can be judged from a consideration of the ratio of the spectral accelerations, surface to base, at different periods. From inspection of all sets of curves, it is clear that the maximum ratio occurs at about 1.3 to 1.4 seconds making this the effective period of the deposit.

Figure 6 provides a comparison of the spectral curves for derived motions with that for recorded motion on rock at Yerba Buena. For additional comparison, bedrock motion for Channel 12 was derived using the traditional SHAKE analysis (i.e., no modification for σ'_{vo}) and its spectral curve is compared with those

for Yerba Buena and the modified SHAKE analysis in Figure 7. It is seen that the already high peak at approximately 0.2 seconds in the modified SHAKE curve is unreasonably high for the traditional SHAKE analysis.

Given the agreement between the recorded rock motion and the deconvoluted spectra shown in Figure 6 and peak rock accelerations (0.12g deconvoluted versus 0.11g recorded maximum peak value on rock in the Bay area), it was decided that the modified SHAKE analysis gives sufficiently accurate free-field stresses and strains to proceed with both the liquefaction and pile stiffness evaluation studies as discussed subsequently.

Figure 8 shows the variation in equivalent shear strain with depth from deconvolution using the modified SHAKE program relative to all horizontal free field motion input. Figure 9, which is a plot of the effective modulus ratio with depth for Channel 3 and 12 input, is an indication of the nonlinearity of the responses induced in the different materials during the Loma Prieta earthquake. A shear modulus ratio of one signifies that the material is responding as an elastic material at its initial tangent shear modulus (G_{max}).

LIQUEFACTION ANALYSIS

Figure 10 indicates the soil layers representative of a longitudinal cross section taken midway across the slope of Figure 11. This is slightly different than the soil layering depicted in Figure 3 which represents conditions at the top of the slope where the free-field instruments are located. As indicated in Figure 11, the 37-ft. thick sand layer located near the top of the profile was allowed to take on different property values corresponding to the assumption of different relative densities (D_r) for the sand. Further, the modulus (G_{max}) and related shear wave velocity (V_s) values were allowed to vary with depth within the layer in relation to the change in the mean normal effective stress.

While the consulted soil reports and borings generally yield a corrected standard penetration test blow count (N_1) value of 70 or greater for this silty sand, an N_1 that corresponds to a Dr of 100%, it is known that both natural and hydraulic fill sand at other locations in the Oakland harbor (some of which liquefied during the earthquake) exhibit dramatically lower blow count values (down to 10 or less). Furthermore, it is this sand layer that provides the support for the wharf piles. Therefore, it was decided to evaluate the possibility of liquefaction at the site for other assumed combinations of D_r and N_1.

Rock motion for Channel 12 (i.e., the greater motion in the long direction of the wharf) was used to assess the equivalent shear stress (τ_{eq}) and, hence, the earthquake induced stress ratio ($R=\tau_{eq}/\sigma'_{vo}$) with depth through this layer for these different density states of the sand: D_r=100%, N_1=70; D_r=90%, N_1=44; D_r=58%, N_1=16; and D_r=40, N_1=6. Figure 12 shows the variation in stress ratio with depth through the sand as obtained from a modified SHAKE analysis. Realize, of course, that changes in the property values for the sand cause changes in the resulting near-surface response (i.e., strain, acceleration, etc.).

Superposed on the plot are vertical lines of the stress ratio necessary to cause liquefaction in four equivalent cycles of shaking for different N_1 and D_r values. While four equivalent cycles of excitation is a low value for the

typical magnitude 7 earthquake, this is the value assessed from the Channel 12 surface acceleration record using the weighting techniques after Seed et al. (1975).

The stress ratios to cause liquefaction were established from curves presented by Norris (1988) which are cross plotted from those given by Seed et al. (1983). Corrections relating to the percentage of fines derived from the relations presented by Seed et al. (1984), applied to the Norris (1988) curves, give the curves shown in Figure 13. Such treatment of fines is important in the present case because the near surface sand is silty. Table 1 presents the values to cause liquefaction in four cycles for various combinations of N_1 and percent fines. Only the values immediately bracketing the variation in induced stress ratio are shown in Figure 12.

It is clear from Figure 12 that, regardless of the difference in variation in induced stress ratio (i.e., for different N_1 and D_r combinations), clean sand with an N_1<25 to 30 blows (D_r<75 to 80%) or silty sand with an N_1<20 blows (D_r<70%) with between 15 and 35% fines would have liquefied had it been present in any form at this location (i.e., layer, seam or lens). This is undoubtedly what happened in areas immediately surrounding the instrumented wharf. On the other hand, at this level of density (70-85%) and above it is unlikely that there would have been any significant softening of the sand during the course of the Loma Prieta earthquake, i.e., any pore pressure buildup causing possibly greater slope or foundation movement would have been accompanied by a dilatant reaction that would have arrested any significant realization of such deformation. Therefore, either the sand was perfectly stable and not likely to soften or it would have liquefied.

PILE FOUNDATION STIFFNESSES

Figure 11 shows the vertical and batter piles used to support the wharf. These are driven 18-in. square prestressed concrete piles. There are approximately 1000 piles over the 1600 ft. length of the wharf. The spacing between the piles varies but it large enough that the piles can be considered as isolated (i.e., there is no group reduction factor to consider). Further, the piles have very little dead load to support and the tip load mobilized at the lower loads is so small that the piles can be considered symmetric as far as their axial response (tension versus compression) is concerned.

The nonlinear variation in vertical stiffness (at groundline) shown in Figure 14 was derived from similar shaped load-settlement curves from three pile load tests (two on piles from Row E and one on a pile from Row B) conducted at the time of construction. Superposed on this curve is a line of constant stiffness of 2000 kips/in which corresponds to the level of shear modulus and strain due to the free-field motions. In other words, due to the earthquake, the shear modulus in the supporting sand layer is already reduced to a certain level and the shear modulus of the soil would not be any higher than the (reduced) free-field value even if the vertical interaction displacements were less than the associated 0.03 in. value. Alternatively, when the interaction displacements and associated shear strains are higher, the soil shear modulus is lower and the vertical pile stiffness is governed by the inertial interaction response.

Using a laterally loaded pile analysis program by Gowda (1991), the lateral

stiffness of the piles was assessed over a wide range in deflection. The curves of Figure 15 are for groundline response for the moment condition of the lateral load applied at the deck times the unsupported length of the pile. One and one-half ft. of Bay Mud (undrained shear strength S_u=1440 lbs/ft^2) over dense sand (friction angle ϕ=39^o) was assumed for this analysis. The superposed cutoff for free-field conditions is not shown but would occur at a groundline inertial interaction or relative deflection of less than 0.02 in. This is smaller than the relative lateral deflections that derive from the dynamic analysis of the wharf described in the next section.

It should be noted that the batter piles were treated as if they have normal and axial stiffnesses equal to the lateral and axial stiffnesses of vertical piles of the same embedment and unsupported length.

Given the high relative density of the supporting sand layer, it was deemed that the above stiffnesses would apply during the earthquake, i.e., there would be no softening of the stiffness curves due to developing porewater pressures in the sand. This would not be the case if the blow count or relative density of the layer were lower than, say, N_1=20 or D_r=70%, but then as shown in the last section such sand would liquefy directly. Of course it may be that at other locations the sand is nonuniform and might liquefied locally without yielding a mechanism for slope failure. Therefore, there might be a momentary reduction in stiffnesses. More detrimental would be the loss of sand strength at shallow depth immediately below the thin cover of Bay Mud causing a significant reduction in lateral (as compared to vertical) stiffness and, hence, a greater transfer of lateral load to the batter piles.

DYNAMIC ANALYSIS OF THE WHARF

The program IMAGES-3D (Leung, 1988) was used for the dynamic analysis of the wharf. A repeatable 48-ft. long by 62-ft. wide section of the deck and supporting piles was modeled with brick elements (for the deck) and three-dimensional beam elements (for the pile). Lateral (two directions) and axial spring stiffnesses were assigned at groundline corresponding to the level of assumed (maximum) relative displacements. The stiffnesses were then changed in successive runs until displacement compatible values from the curves of Figures 14 and 15 were obtained. This takes a couple of iterations; but, unless it is done, it cannot be said that the proper distribution of the loads to the structure has been achieved. It should be noted that the pile connection at the deck was handled by embedding a beam element in the brick (deck) element.

A modal analysis was performed to establish the frequencies, mode shapes, modal weights and participation factors of the modeled wharf. Only the first three modes were considered in the dynamic analysis. Damping was taken constant in all modes at a value of 5%, a reasonable value for elastic analysis of reinforced concrete structures. The transverse response of the structure was evaluated based on Channel 1 free-field motion input. Figure 16 is a comparison of computed (Node 18) and recorded (Channel 4) accelerations. Similar good comparison was achieved between Node 34 and Channel 5.

The peak relative displacements at groundline for piles of the different rows varied as follows: 4.16 in. lateral maximum for piles of Row A to a minimum peak value of 0.02 of piles of Row C (outboard); and 0.022 in. axial displacement

for piles of Row D to).0006 in. displacement for piles of Row A.

Channel 12 motion was input to the model to ascertain the response had the incoming motions or the orientation of the wharf been reversed. The computed response at Node 18 for the reversed motion is about the same as that for the actual input.

Based on the above analysis the peak shear forces at the pile head of the batter piles varied from 23.7 to 15.3 kips for the true input (Channel 1) and from 15.4 to 9.2 kips for the reversed input (Channel 12). These shear loads are well within that allowed and would not cause damage to the piles. Therefore, the piles damaged at other locations were likely embedded in a nonuniform sand deposit where liquefaction occurred locally below the thin cover of Bay Mud thus causing reduced lateral stiffness and, hence, even greater transfer of lateral force to the batter piles. This hypothesis is still to be tested but it can be accomplished in a straightforward manner by simply reducing the lateral/normal stiffness of all piles to a very low value (say, 0.5 kip/in) while maintaining compatible vertical stiffnesses. The resulting shear loads at the heads of the batter piles will indicate whether this was a likely mechanism for damage.

CONCLUSIONS

The current study has been useful in looking at free-field motion, soil-foundation interaction response and foundation-structure behavior. However, the dramatic response that occurred at nearby facilities seemed far from developing at the instrumented Oakland Outer Harbor Wharf due largely to the high relative density of the near-surface sand in which the piles supporting the wharf are founded. Simply assuming a lower density of the whole layer will not explain the likelihood for pile damage because the induced stress ratio in the layer is so large that the sand would need to be of such high density (D_r>70%) to survive liquefaction that it would not be subject to softening due to developing porewater pressures. Alternatively, a mechanism of damage arising from a loss in lateral stiffness due to local near-surface liquefaction is still being investigated. There was no particular effect due to a change in the orientation of the incoming motions. In total, the present study has shown the usefulness of the CSMIP records in the attempted verification of methodologies for soil-foundation-structure interaction analysis; though, at the instrumented Oakland Outer Harbor Wharf, there was nothing of dire consequence to report. Basically, the structure was of such small mass that, in such competent soil, there was no significant interaction response, i.e., the structure was forced to follow free-field soil motion.

ACKNOWLEDGEMENTS

This study was supported by a grant from the Office of Strong Motion Studies of the Division of Mines and Geology of the California Department of Conservation. The authors would also like to thank Jerry Serventi of the Port of Oakland, Dave Rogers of Rogers Pacific, Dick Short of Kaldveer, Bob Darrah of Dames and Moore, Mark Best of Pioneer Drilling, and Ad Goldschmidt of CALTRANS for providing a variety of information (soil reports, boring logs, pile load test results, driving records, etc.) relative to the Oakland harbor and Cypress area.

REFERENCES

1. Gowda, P. (1991), "Laterally Loaded Pile Analysis for Layered Soil Based on the Strain Wedge Model," M.S. Thesis, University of Nevada, Reno, in preparation.

2. Hardin, B.O., and Drnevich, V.P. (1972), "Shear Modulus and Damping in Soils: Design Equations and Curves," Journal of Soil Mechanics and Foundations Division, ASCE, Vol. 98, No. SM7, pp. 667-692.

3. Leung, W.H. (1988), "IMAGES-3D: Interactive Microcomputer and Graphics of Engineering Systems-3 Dimensional," Celestial Software, Inc., Berkeley, California.

4. Norris, G.M. (1988), "Liquefaction of the Meloland Overcrossing During the Imperial Valley Earthquake of 1979," Bulletin of the Association of Engineering Geologists, AEG, Vol. XXV, No. 2, pp. 235-247.

5. Seed, H.B. and Idriss, I.M. (1970), "Soil Moduli and Damping Factors for Dynamic Response Analyses," Report No. EERC 70-10, Earthquake Engineering Research Center, University of California, Berkeley.

6. Seed, H.B., Idriss, I.M., and Arango, I. (1983), "Evaluation of Liquefaction Potential Using Field Performance Data," Journal of the Geotechnical Division, ASCE, Vol. 109, No. 3, March, pp. 458-482.

7. Seed, H.B., Idriss, I.M., Makdisi, F., and Banerjee, N. (1975), "Representation of Irregular Stress Time Histories by Equivalent Uniform Stress Series in Liquefaction Analyses," Report No. EERC 75-29, Earthquake Engineering Research Center, University of California, Berkeley.

8. Seed, H.B. and Sun, J.I. (1989), "Implications of Site Effects in the Mexico Earthquake of Sept. 19, 1985 for Earthquake-Resistant Design Criteria in the San Francisco Bay Area of California," Report No. UCB/EERC-89/03, Earthquake Engineering Research Center, University of California, Berkeley.

9. Seed, H.B., Tokimatsu, K., Harder, L.F.,and Chung, R.M. (1984), "The Influence of SPT Procedures in Soil Liquefaction Resistance Evaluations," Report No. UCB/EERC-84/15, Earthquake Engineering Research Center, University of California, Berkeley.

10. Schnabel, P.B., Lysmer, J., and Seed, H.B. (1972), "SHAKE: A Computer Program for Earthquake Response Analysis of Horizontally Layered Sites," Report No. EERC 72-12, Earthquake Engineering Research Center, University of California, Berkeley.

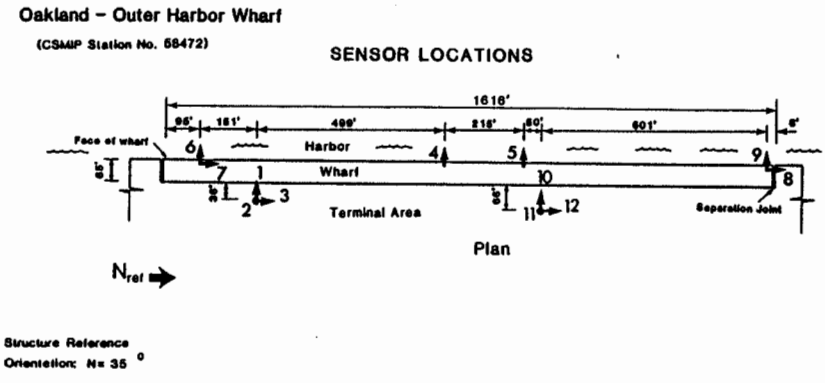

Fig. 1 Sensor location at Oakland Outer Harbor Wharf

18'	Sand	σ'_{vo} = 563 psf	V_s = 500 ft/sec
4'	Clay	1226	350
43'	Sand	2671	1100
80'	Clay	6035	1000
20'	Clay	8560	1200
65'	Clay	10706	1200
25'	Clay	12978	1200
45'	Clay	14746	1400
85'	Sand	18538	1750
15'	Clay	21573	1250
95'	Sand	24921	1750
Half Space (Franciscan Greywacke)			V_s = 2000 ft/sec

Fig. 2 Soil profile used for one-dimensional deconvolution studies

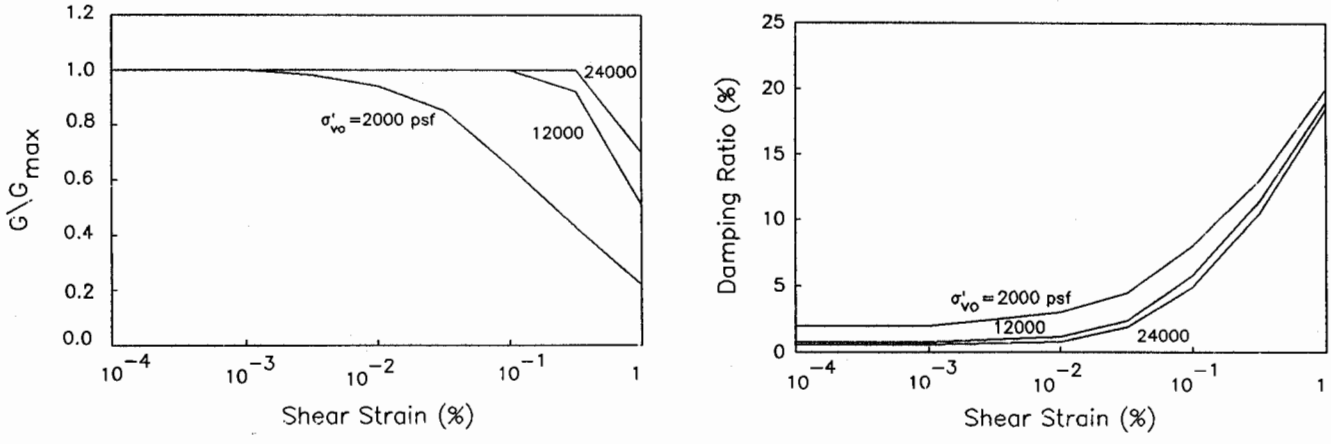

Fig. 3 Shear modulus reduction and Damping curves for Bay Mud for different σ'_{vo}

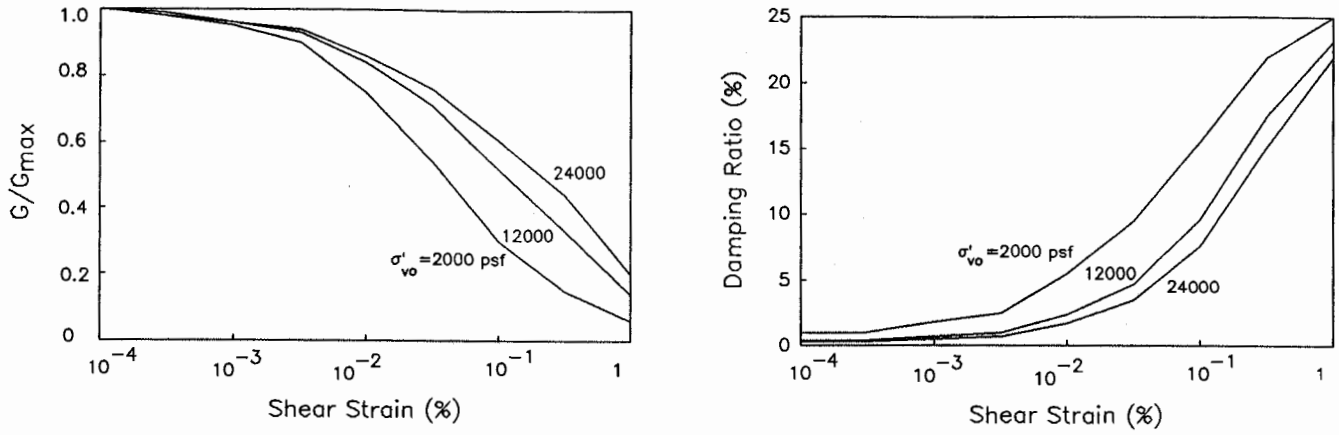

Fig. 4 Shear modulus reduction and Damping curves for sand for different σ'_{vo}

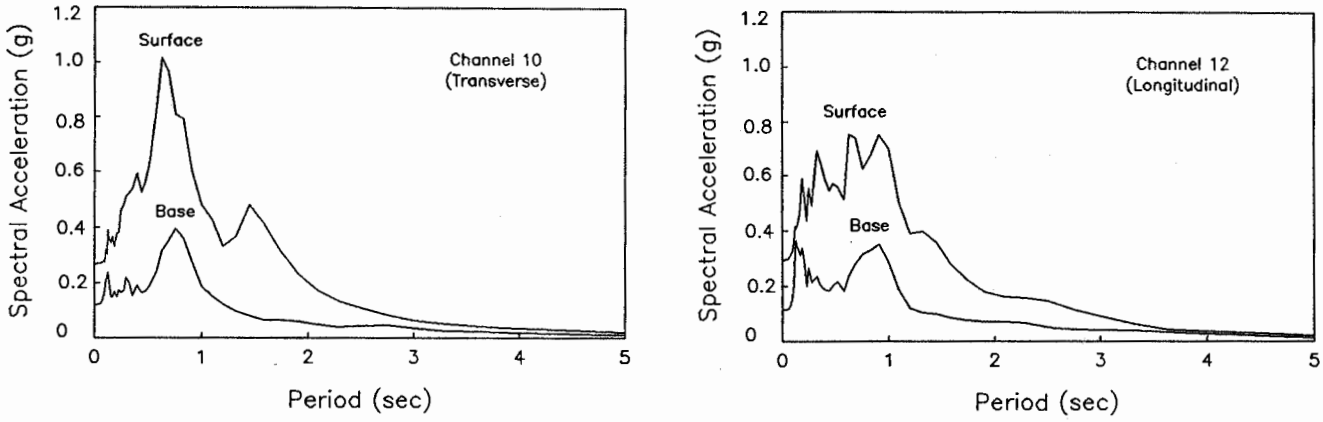

Fig. 5 Surface and (deconvoluted) rock spectral acceleration curves, Channel 10 & 12

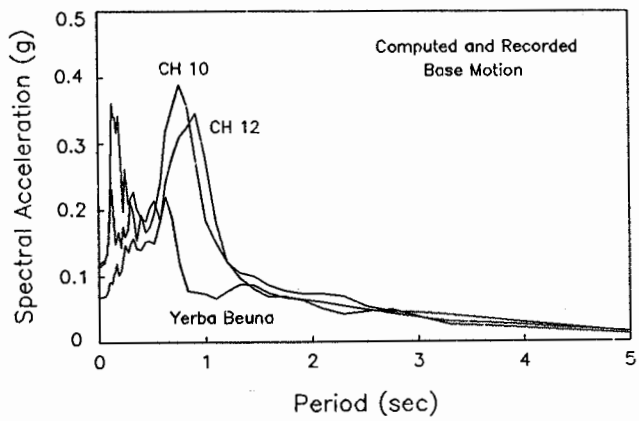

Fig. 6 Spectral acceleration curve for rock motions, Channels 10 & 12 and Yerba Buena

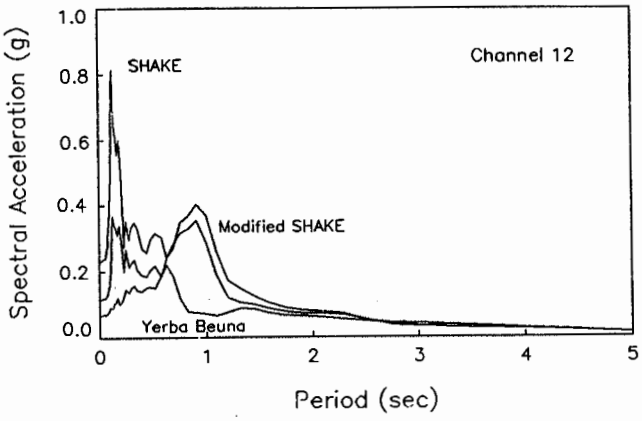

Fig. 7 Spectral acceleration curves for rock, Channel 12 modified SHAKE vs. traditional SHAKE analysis and Yerba Buena

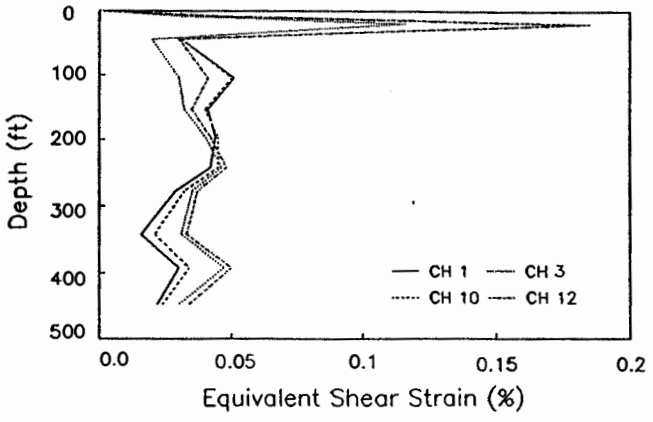

Fig. 8 Variation in equivalent shear strain

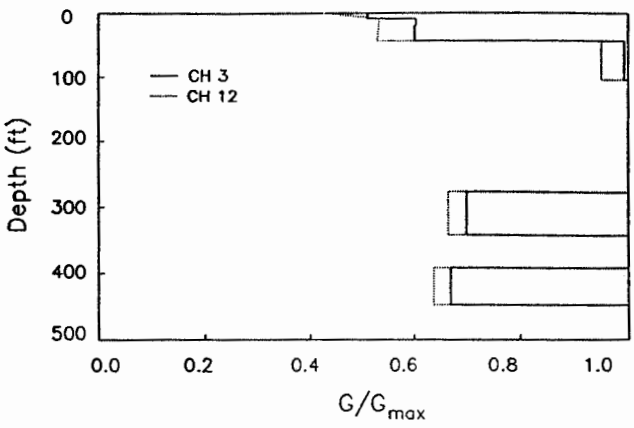

Fig. 9 Variation in modulus reduction

15'	Clay	σ'_{vo} = 1226 psf	V_s = 500 ft/sec
37'	Sand	2671	Variable
80'	Clay	6035	1000
20'	Clay	8560	1200
65'	Clay	10706	1200
25'	Clay	12978	1200
45'	Clay	14746	1400
85'	Sand	18538	1750
15'	Clay	21573	1250
95'	Sand	24921	1750
Half Space (Franciscan Greywacke)			V_s = 2000 ft/sec

Fig. 10 Soil profile taken and slope for liquefaction studies

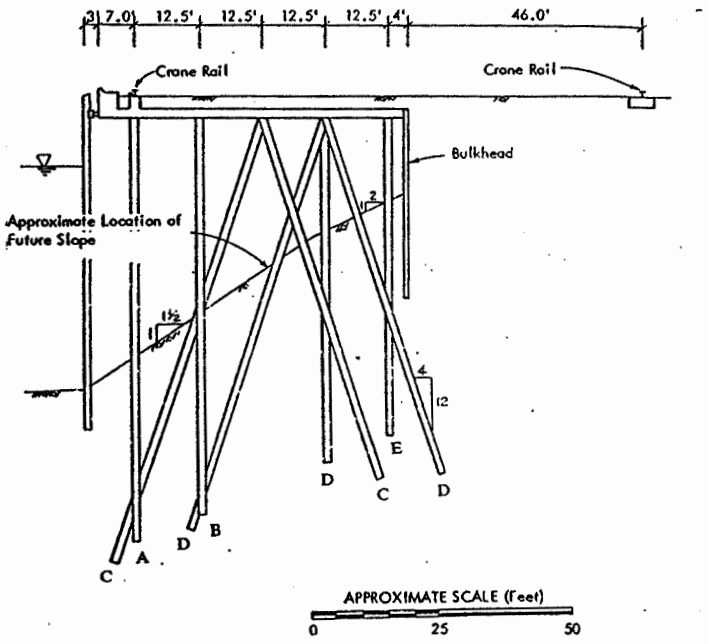

Fig. 11 Pile arrangement

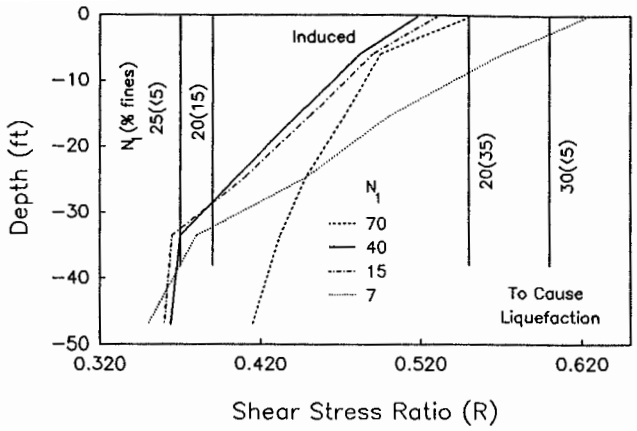

Fig. 12 Variation in stress ratio R for Channel 12 motion

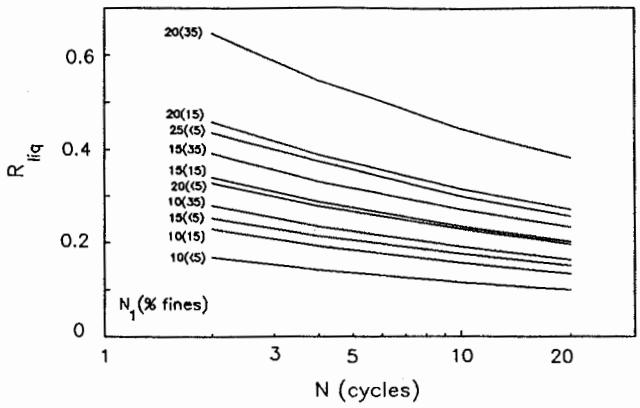

Fig. 13 Liquefaction Curves

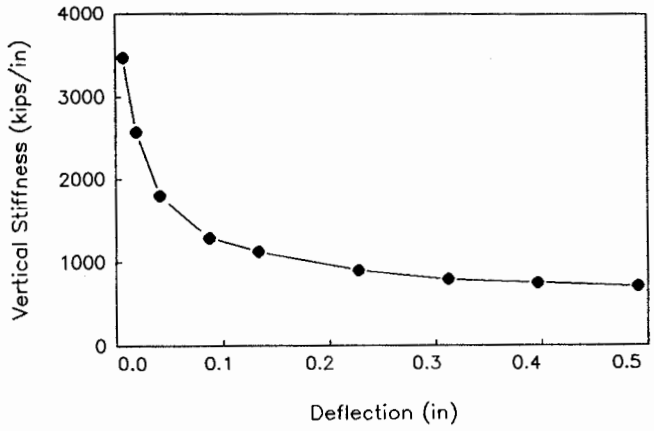

Fig. 14 Axial stiffness variation, all piles

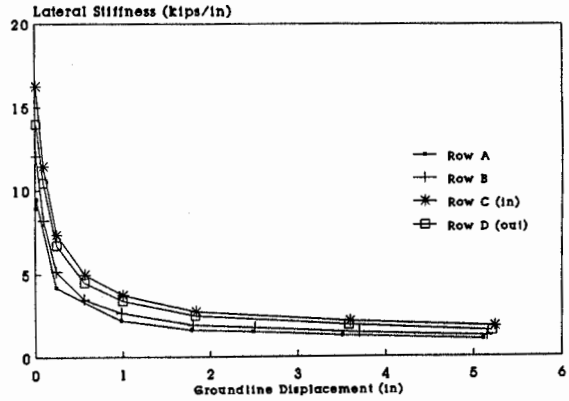

Fig. 15 Lateral stiffness variation, piles of Row A, B, C, D (Others not shown)

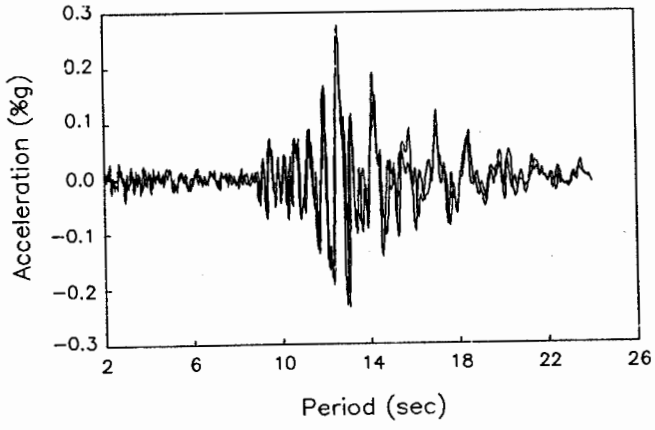

Fig. 16 Computed (Node 34) using Channel 1 input versus recorded (Channel 5) accelerations on the wharf

Table 1. Stress Rate to Cause Liquefaction in Four Cycles for Different Blow Counts and Percent Fines

N_1 blows (% fines)	R_{liq}
25(≥15)	∞
30(≤5)	≈0.6
20(35)	.55
20(15)	.39
25(≤5)	.37
15(35)	.33
20(≤5)	.29
15(15)	.28
10(35)	.23
15(≤5)	.21
10(15)	.19
10(≤5)	.14